COMPARISON BETWEEN STOKES DRIFT AND WIND-INDUCED SLIP OF MEDITERRANEAN DRIFTERS

Arthur Prigent[1, 3], Pierre-Marie Poulain[1], Milena Menna[1], Giovanni Besio[2]

[1]Istituto Nazionale di Oceanografia e di Geofisica Sperimentale (OGS),
Trieste, Italy

[2] DICCA -Università degli Studi di Genova,
Genova, Italy

[3] Ecole Nationale Supérieure de Techniques Avancées Bretagne (ENSTA Bretagne),
Brest, France

Approved for release by: ……

Dr. Paola Del Negro
Director, Oceanography Section

Table of Contents

1. Introduction 3
2. Drifter designs 3
a) CODE drifters 3
b) SVP drifters 4
c) Positioning and data telemetry 4
3. Datasets 4
a) Data processing 4
b) Drifter datasets 5
c) Wind products 5
4. Analysis on the Stokes Drift formula 5
5. Wave model data 7
6. Stokes drift velocities in the Mediterranean Sea 9
7. Interpolation of the wave model at the drifter positions 12
8. Estimation of drifter downwind slip 12
9. Study on the Stokes drift velocities 16
10. Conclusions 18
11. References 19

1. Introduction

Over the years, several studies of the impact of the Stokes drift on the trajectories of objects drifting on the sea surface were made (see for instance Heath, 2011; Wang et al, 2014). Generally, the Stokes drift velocity is defined as the difference between the average Lagrangian flow velocity of a fluid parcel, and the average Eulerian flow velocity of the fluid at a fixed position. As an example, a particle floating at the free surface of the water waves experiences a net Stokes drift velocity in the direction of wave propagation. In the case of this study, the particles are drifters. The aim of this report is to compare the Stokes Drift velocities with the slip induced by the wind on the trajectories of surface drifters in the Mediterranean Sea. In order to study these effects, the data from different types of drifters were used. Surface Velocity Program (SVP) drifters drogued at 15-m nominal depth and undrogued (Sybrandy and Niiler, 1991), as well as Coastal Ocean Dynamics Experiment (CODE) drifters (Davis, 1985) datasets were used to estimate the impact of the Stokes drift on the drifter trajectories. In section 2, the drifters used for the study are described. Section 3 gives information on the datasets used for this study. In section 4. the method to compute Stokes drift velocities is described. Section 5 focuses on the wave model used to compute the Stokes drift velocities at the drifter positions. An estimation of the Stokes drift velocities in the Mediterranean Sea is given in section 6. The interpolation of the Stokes drift data is presented in section 7. Section 8 focuses on the study of the downwind slip. Results of the Stokes drift velocities are analyzed in section 9. Conclusions are included in Section 10.

2. Drifter designs

a) CODE drifters

The CODE drifter (Davis, 1985) was designed as an inexpensive water follower to track currents in the upper meter of the oceanic mixed layer. The CODE drifters' "X" shaped sail patterns catch the surface layer water currents like a sail catches the wind. The CODE drifters mostly used in this study were manufactured by Technocean (model Argodrifter). It is a Lagrangian drifter which can report position via the Argos satellite-based data collection system. The CODE drifter is a tube, around the central core on top and bottom are eight spring loaded arms which upon deployment from two intersecting orthogonal, vertical, planes made of cloth with an area

approximatively 1 meter square (the central tube forming the vertical axis). Four ball-shaped foam floats tethers from the outer ends of the upper arms. These floats provide the net positive buoyancy to the unit.

b) SVP drifters

SVP drifters (Sybrandy and Niiler, 1991) are the standard design of the GDP. It is also a Lagrangian current-following drifter, designed to track water currents (15 meters depth) beneath the ocean surface. The SVP drifters used in this study are the mini-SVP designs. SVPs consist of a surface buoy that is tethered to a holey sock drogue that is centered at 15 meters depth. A tension sensor, located below the surface buoy where the drogued is attached, indicates the presence or absence of the drogue.

c) Positioning and data telemetry

Two systems were used to track the drifters. The first one is the Argos Data Collection and Location (DCLS) system dedicated to environmental monitoring. This system is based on the Doppler-Fizeau effect, which reflects the shift in frequency of the sound wave or electromagnetic wave when the source of transmission and an observer are in motion relative to each other. Each time it receives a message, the Argos system measures the frequency and the arrival date. Knowing the velocity and the arrival date, the distance between the drifter and the satellite can be computed. This operation done with at least 4 satellites allow us to determine the drifter positions. The second system is Iridium, which is a global full ocean coverage bidirectional satellite communication network. This network is composed of 66 active satellites used for worldwide data communication. The buoy utilizes the network to communicate and transmit essential scientific data.

3. Datasets

a) Data processing

The data processing used is described in Poulain et al. (2004). Here a short summary is given. First the data of each drifter was read, reduced and edited in order to remove outliers and spikes. Then, the despiked data were interpolated onto regular intervals using the kriging analysis technique (Hansen and Herman 1989; Hansen and Poulain, 1995). The edited data from the drifters were interpolated at regular 2-hour intervals using the kriging technique. The interpolated data were then low-pass filtered with a designed filter cut-off period at 36 hours (-3 dB at 36

hours and -49 dB at 27 hours) in order to remove high frequency current components. Finally the low-pass time series were subsampled every 6 hours and the velocities were computed by finite-centered differencing the 6-hourly interpolated-filtered latitude and longitude data.

b) Drifter datasets

The drifter data used in this study cover the whole Mediterranean Sea (30°-46°N, -6°-36°E). The tracking of the drifter was done by the Argos Data Collection and by the Iridium network. The drifter observations are grouped into three datasets. The first dataset is composed of the 767 CODE drifters spanning the period 1986-2017 (Figure 1a). The second dataset is composed of 495 drogued SVP drifters spanning the period 2005-2017 (Figure 1b) among which 176 SVP drifters have lost their drogue. These 176 undrogued drifters are included in the third dataset (Figure 1c).

c) Wind products

The Cross-Calibrated Multi-Platform (CCMP) Ocean Surface Wind Vector Analyses (Atlas et al., 2011) provide a consistent, gapfree long-term time-series of ocean surface wind vector from July 1987 through 2017. The CCMP datasets combine cross calibrated satellite winds using a Variational Analysis Method (VAM) to produce a high resolution (0.25 degree) gridded analysis. The times series of wind (NOAA in this report) were downloaded from the NOAA website (ERDDAP- NOAA/NCDC Blended Daily 0.25-degree Sea Surface Winds – Data Access Form). These products include globally gridded, high-resolution ocean surface vector winds on a global 0.25° grid with a time resolution of 6 hours.

4. Analysis on the Stokes Drift formula

According to Ardhuin and Filipot (2017) an approximation of the Stokes drift velocities in the water column can be computed by the following formula:

$$[U_s, V_s] = \sigma * k * \frac{a^2}{2} * \frac{cosh(2kz + 2kh)}{\sinh^2(kD)} * (cos(\theta), sin(\theta))$$

Equation 1

where *Us* and *Vs* are the Stokes drift velocities respectively in the zonal and meridional directions, a is the wave amplitude, *D* is the mean water depth, *-h* is the depth of the bottom, and $\sigma^2=g*k$ is the dispersion number in deep water. In addition, g is the gravitational acceleration, $k=2*\pi/\lambda$ is the wavenumber, λ is the wavelength, θ is the propagation direction of the waves, *z* is the depth of the computation and *D* is the water depth. Using the deep water approximation the Stokes Drift formula becomes:

$$[U_s, V_s] = \sigma * ka^2 * \exp 2kz * (cos(\theta), sin(\theta))$$

Equation 2

(a)

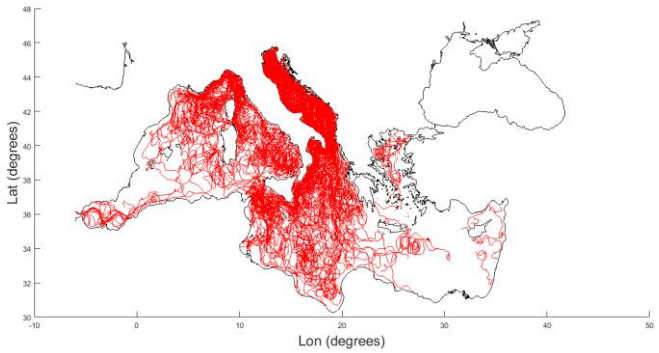

(b)

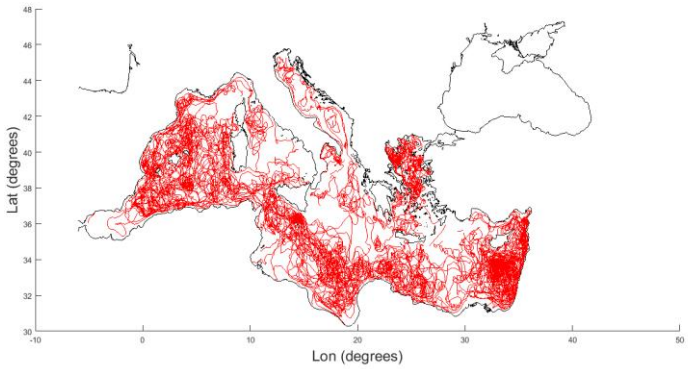

(c)

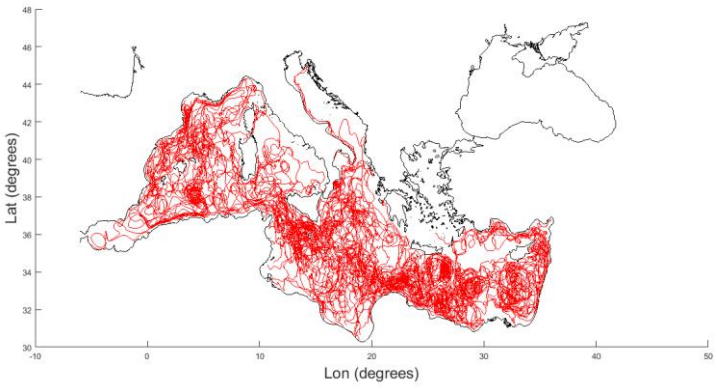

Figure 1. Low-pass-filtered interpolated drifter tracks in the Mediterranean Sea: (a) CODE drifters, 1986-2017; (b) SVP drogued drifters, 2005-2017; and (c) SVP undrogued drifters 2005-2017.

Figures 2a and 2b show the Stokes drift velocities in the water column computed respectively with Equations 2 and 3. Some wave products give the mean period, *Tm*, the mean direction, *θm* and the significant wave height *Hs*. Using these parameters, an approximation of the Stokes drift velocities is computable according to the bulk formula from Kumar et al. (2017):

$$[U_s, V_s] = \frac{Hs^2 w}{16} * \frac{cosh(2kz + 2kh)}{\sinh^2(k * h)} * k * (cos(\theta), sin(\theta)$$

Equation 3

where ω is the angular wave frequency (= *2π/Tm*). Equation 3 has been used to estimate the Stokes drift velocities in the entire Mediterranean Sea using the bathymetry of the basin.

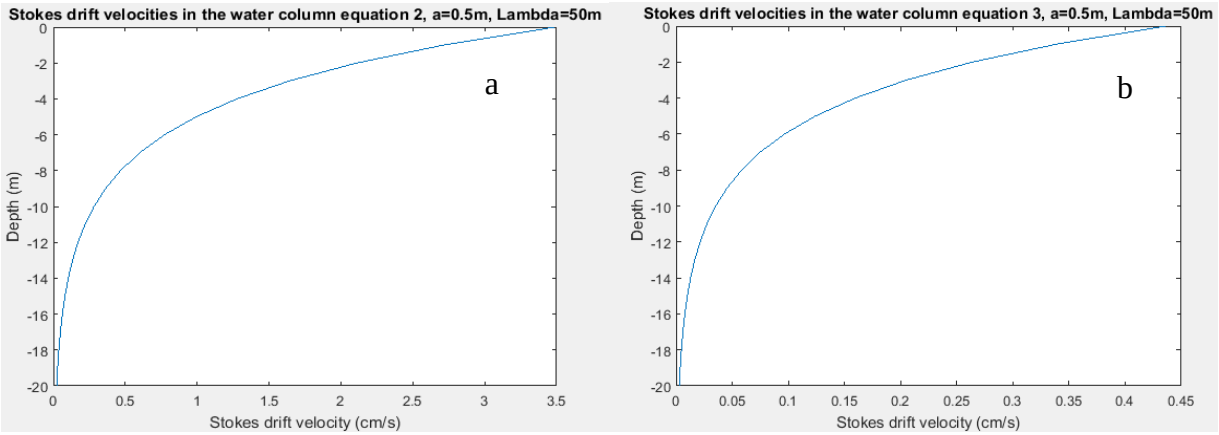

Figure 1. Examples of Stokes Drift velocities in the water column.

5. Wave model data

To estimate the Stokes drift velocities in the water column using Equation 3, the wavelength, *λ=2π/k*, the period, *T=2π/σ*, and the significant height, *Hs*, of the waves are required. Wave characteristics for the Mediterranean Sea have been provided by the Department of Civil, Chemical and Environmental Engineering (DICCA) of the University of Genoa, Italy, that developed a high-resolution wave hindcast in space (0.1°x0.1°) and time (1 hour) for the period

01/01/1979-31/12/2016. The hindcast has been validated and employed for different studies regarding wave climate and analysis (Mentaschi et al., 2013a,b; Mentaschi et al., 2015a,b; Sartini et al, 2015a,b; Besio et al., 2016; Sartini et al., 2016; Besio et al., 2017; Sartini et al., 2017; Masina et al., 2017; Zughayar et al., 2017). Since the wave model has a high resolution, a lower space (1° x 1°) and time resolution of 6 hours were used. Wave hindcast has been produced using the third generation model WAVEWATCH III v3.14 (Tolman et al., 2014). These model results are given on a single grid (Figure 3).The following parameters are available at each grid point:

- YYYY - Year , mm - month , dd - day , HH - hour , MM - minutes , SS - seconds
- Hs - Significant Wave Height [m]
- Tm - Mean Period [s]
- Tp - Peak Period [s]
- Dirm - Mean Direction [°N]
- Dirp - Peak Direction [°N]
- Lm - Mean Wavelength [m]
- Lp - Peak Wavelength [m]
- Wa - Wage age

Using the mean and the peak parameters the Stokes drift velocities were computed at the drifter positions. The Stokes drift velocities have been computed only at the surface (Equation 3) because we assume that drogued SVP drifters (15 m depth) are not influenced by Stokes drift effects. In contrast, CODE and undrogued SVP drifters are influenced by the surface Stokes drift velocities and by wind-driven currents.

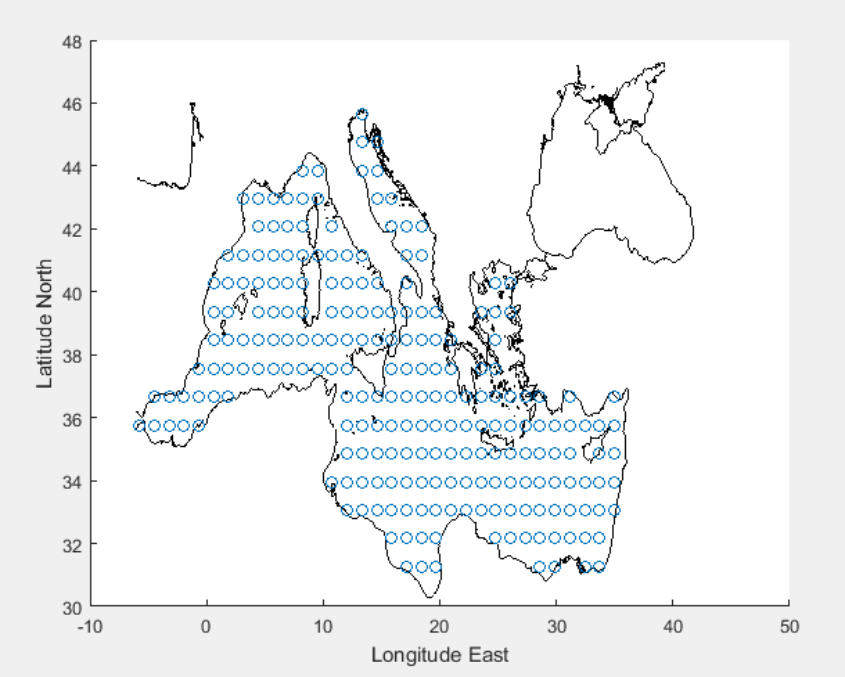

Figure 3. Grid of the wave numerical model.

6. Stokes drift velocities in the Mediterranean Sea

Seeking for a complete study, the maximum Stokes drift velocities for each point of the grid were extracted. This provided us an idea of the magnitude of the Stokes drift velocities in the Mediterranean Sea. Figures 4a and 4b show that the average maximum Stokes drift velocity is around 20 cm/s in the western and in the eastern Mediterranean Sea. We can notice some episodic maximum values around 1 m/s. These results are of the same order of magnitude than those found by Jordà et al. (2007) in the Catalan sea (about 20-30 cm/s).

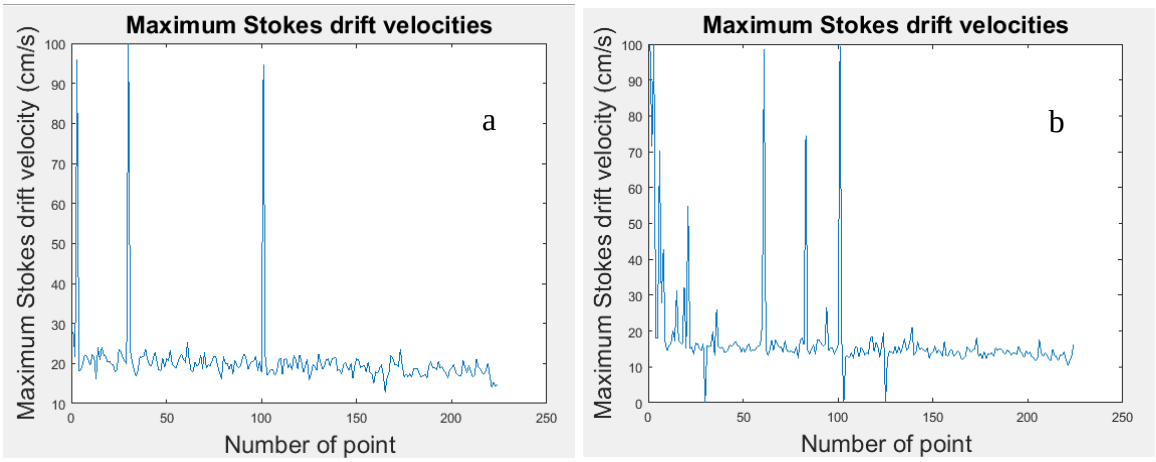

Figure 4. Maximum Stokes drift velocities at each grid point in the western (a) and eastern (b) Mediterrranean.

In order to have a better estimation of the possible Stokes drift velocites in the Mediterranean Sea, histograms of the distribution of the Stokes drift velocites (Figure 5) were produced in two selected areas of the Mediterranean Sea (Figure 6). According to the histograms (Figure 5), Stokes drift velocities are ranging between 0 and 20 cm/s in Mediterranean Sea without taking into account the maximums. In addition, in the western basin area (Figure 5a and 5b) the Stokes drift velocities are a bit higher than in the eastern basin area (Figure 5c and 5d). This makes sense since the surface wave field is more energetic in the western Mediterranean than in the eastern basin.

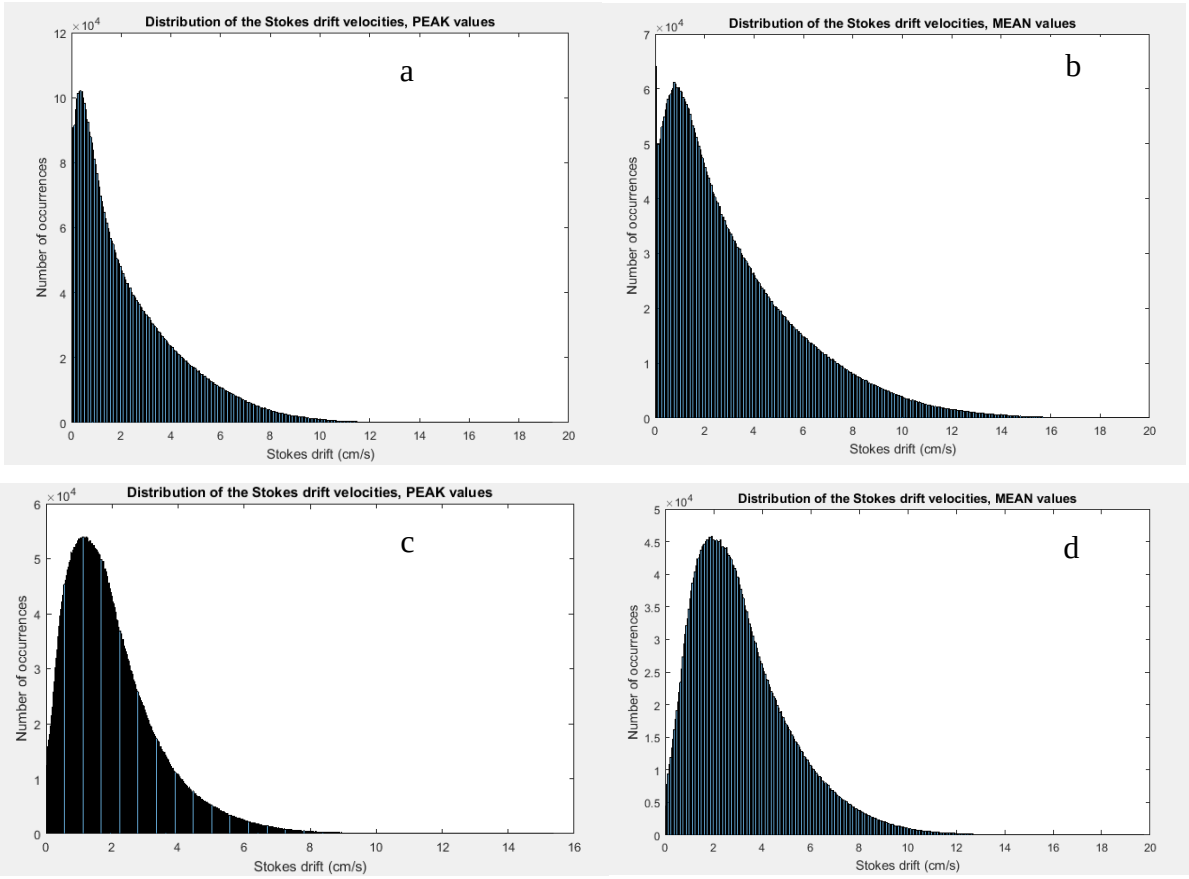

Figure 5. Histograms of the Stokes drift velocities in the western (a and b) and eastern (c and d) Mediterranean basins. Peak (left) and mean (mean) wave parameters were used.

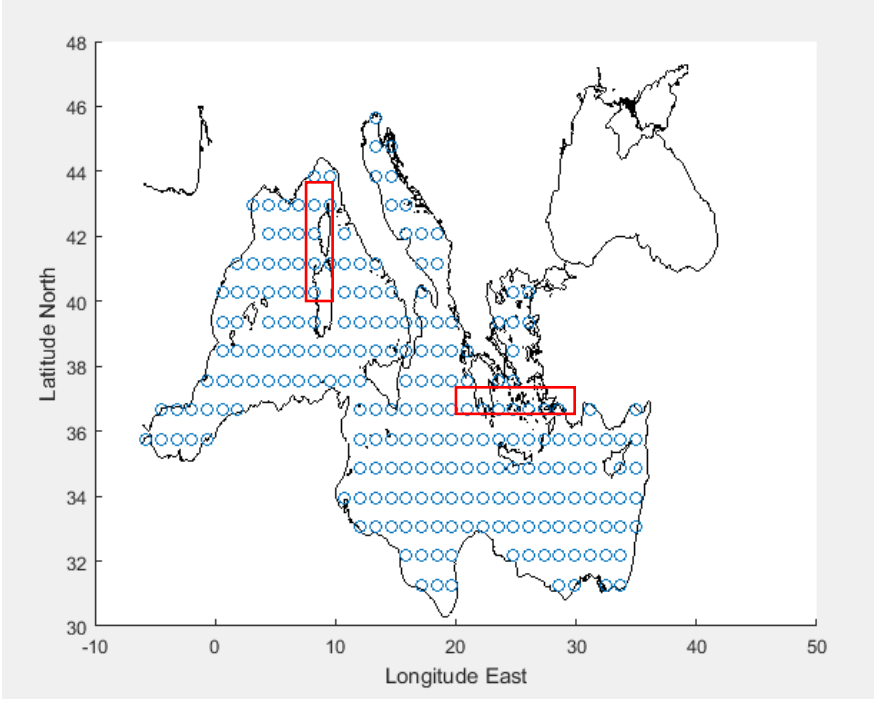

Figure 6. Areas used for the study of the distribution of the Stokes drift velocities.

7. Interpolation of the wave model at the drifter positions

A Matlab bilinear interpolator, interp2 with the method nearest, was used to compute the velocities at the drifter positions using Equations 2 and 3. According to the results of the interpolation, Equation 2 seems to overestimate the Stokes drift velocities. Indeed, this equation produces some Stokes drift velocities larger than 30 cm/s, which is barely possible according the distributions (Figures 5). Thus, the following study was focused on the results given by Equation 3.

8. Estimation of drifter downwind slip

The wind-driven currents were extracted from the CODE and SVP (undrogued - *Usvpl* and drogued - *Usvp*) velocities using the following regression models:

$$U_{CODE} = \alpha_1 + \beta_1 W_{CODE} + error$$
$$U_{SVP} = \alpha_2 + \beta_2 W_{SVP} + error$$
$$U_{SVPL} = \alpha_3 + \beta_3 W_{SVPL} + error$$

Equation 4

These models were computed with two different wind products, one from the NOAA and the one from CCMP. The computations with the two different models allow us to validate the results.

Furthermore, the offset of the regression models (Equation 4) αi were forced to zero to seek a simple linear relationship between drifter and wind velocities. The results are listed in Table 1. Using 154000 6-hourly observations in the whole Mediterranean Sea, the wind-driven currents measured by the CODE drifters appears to be about 0.84% of the wind speed at an angle of 29° to the right of the wind vector. These results are similar to those of Poulain et al. (2009) using 46000 observations. This simple linear relationship explain up to 11% of the variance for the CCMP wind model and up to 10% for the NOAA model.

The drogued SVP drifter velocities (133875 6-hourly observations) are less correlated with the winds. The regression models explains only 4.6% (NOAA) and 5.3% (CCMP). The slope of the regression model is about 0.5% of the wind speed and the veering angle of the drifter-inferred currents with respect to the winds ranges between 39 and 43° to the right of the wind vector.

When the SVP drifter have lost their drogue (37006 six-hourly observations) the correlation with the wind is much higher. Indeed the coefficient of determination reaches 31%. The linear model gives a slope of about 1.6% whereas it was found 1.8% in 2009, with a veering angle to the right of the wind of 19°.

Model	α	β	R^2	N
CCMP				
$U_{CODE} = \alpha + \beta W$	$0.162exp(-157.8i)$	$0.0084exp(-29.0i)$	11.4	154389
$U_{CODE} = \beta W$		$0.0084exp(-29i)$	11.4	154389
$U_{SVP} = \alpha + \beta W$	$0.17exp(117.6i)$	$0.005exp(-42.8i)$	4.9	133875
$U_{SVP} = \beta W$		$0.0052exp(-43.1)$	4.9	133875
$U_{SVPL} = \alpha + \beta W$	$0.31exp(83.7i)$	$0.016exp(-19.3i)$	30.7	37006
$U_{SVPL} = \beta W$		$0.016exp(-19.0)$	30.7	37006
NOAA				
$U_{CODE} = \alpha + \beta W$	$0.076exp(-123.7i)$	$0.0073exp(-22i)$	9.8	112558
$U_{CODE} = \beta W$		$0.0073exp(-22i)$	9.8	112558
$U_{SVP} = \alpha + \beta W$	$0.17exp(-114i)$	$0.0049exp(-39.0i)$	4.2	123197
$U_{SVP} = \beta W$		$0.0049exp(-39.4)$	4.2	123197
$U_{SVPL} = \alpha + \beta W$	$0.25exp(96i)$	$0.014exp(-17.6i)$	23.2	35456
$U_{SVPL} = \beta W$		$0.015exp(-16.6)$	26.7	35456

Table 1 Results of the linear regression models used to estimate wind-driven currents measured by CODE (Ucode) and SVP (Usvp and Usvpl) drifters.

In order to compare the influence of the Stokes drift with the wind-induced currents on the drifter trajectories a study of the wind is needed. To estimate the slippage of undrogued drifters, pairs of drifter observations satisfying the following conditions were sought in the drifter dataset: 1) one observation is provide by a drogued SVP drifter, and the other by an undrogued SVP drifter; 2) the two observations should be simultaneous; and 3) the two drifters should be separated by less than 20 km (Figure 7a) or 40 km (Figure 7b). Linear regression models (Equation 5) were applied to the drifter observations and wind product in the Mediterranean Sea.

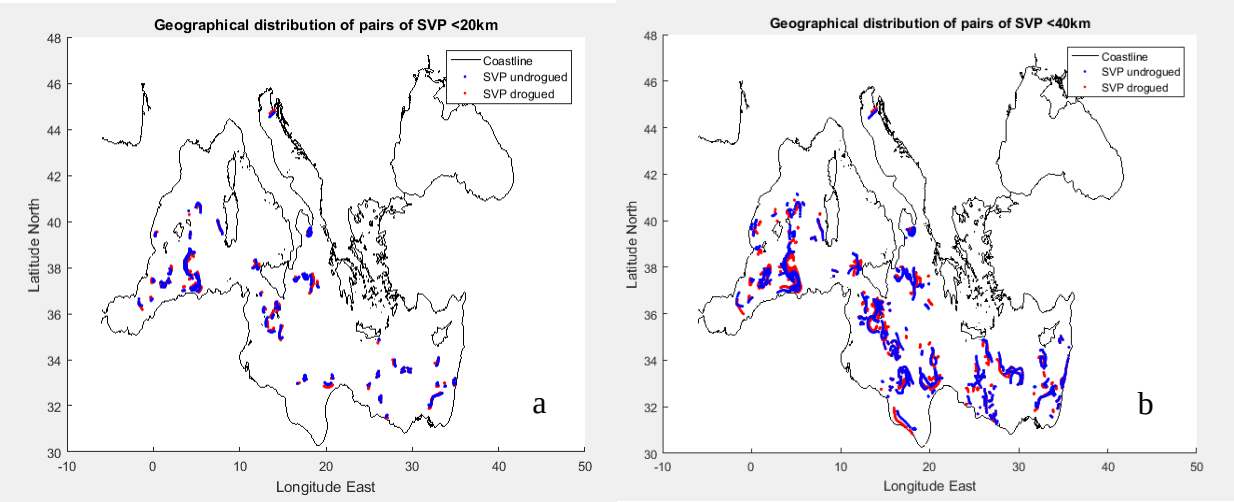

Figure 7. Pairs of drogued and undrogued SVP drifters separated by less than 20 km.

Several regression models were applied to the nearly collocated (distance < 40 km) and simultaneous undrogued (*Usvpl*) and drogued (*Usvp*) SVP velocities as a function of wind (*W*) (see Table 2) as it was done in Poulain et al. (2009). Using 2374 pairs with drifter observations separated by less than 40 km compared to the 771 pairs of 2009 the results have been updated.

$$U_{SVPL} = \alpha + \beta U_{SVP} + \gamma W$$

$$(U_{SVPL} - U_{SVP}) = \beta W$$

$$(U_{SVPL} - U_{SVP})_{downwind} = \beta |W|$$

Equation 5

Taking the same regression models (Equation 5), the velocity difference between undrogued and drogued SVP drifters follows a model with a slope of 0.014 and a small veering to the right of 18.5°. This model explains only about 1.5% of the variance of the velocity difference. As the veering angle is small, we can assume that the response is essentially downwind. The explained variance for the downwind model is the same. In order to compare the drogued and undrogued drifters with better collocated pairs the maximal distance has been reduced to 20 km. The quantity

of pairs is obviously reduced (754) but still five times larger than the data available in 2009 (only 164 pairs). The downwind slippage is 1.4% and explains 16% of the variance.

The scatter diagram of downwind slippage versus wind speed is depicted in Figure 8 along with the regression lines corresponding to the models using pairs separated by less than 40 and 20 km. Downwind slippage speeds can be as large as 70 cm/s for wind speed ranging in 0-18 m/s. Using pairs separated by less than 20 km yields slippage estimates ranging between -40 and +40 cm/s.

Model	$\alpha(cm/s)$	β	γ	R^2	N(Dist,km)
CCMP					
$U_{SVPL} = \alpha + \beta U_{SVP} + \gamma W$	2.84	$0.14exp(-36.2i)$	$0.017exp(-18.6i)$	11.7	2374(40)
$U_{SVPL} = \alpha + \beta U_{SVP} + \gamma W$	2.5	$0.26exp(-44.9i)$	$0.016exp(-11.0i)$	9.4	757(20)
$(U_{SVPL} - U_{SVP}) = \beta W$		$0.014exp(-18.5i)$		16.5	2374(40)
$(U_{SVPL} - U_{SVP}) = \beta W$		$0.013exp(-11.0i)$		14.2	757(20)
$(U_{SVPL} - U_{SVP})_{downwind} = \beta \lvert W \rvert$		0.014		16.6	2374(40)
$(U_{SVPL} - U_{SVP})_{downwind} = \beta \lvert W \rvert$		0.012		14.3	757(20)

Table 2. Results of the linear regressions on CODE and SVP drifters.

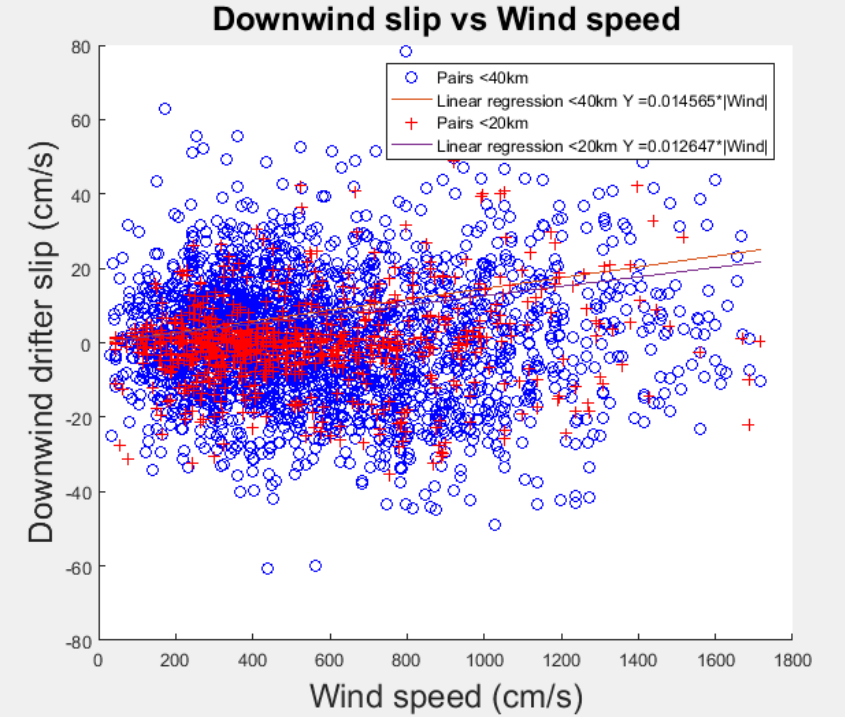

Figure 8. Scatter diagram of downwind slip vs wind speed. Plus signs and circles correspond to pairs separated by less than 20 km and 40 km, respectively.

CODE and SVP drifters data in the entire Mediterranean Sea were used in concert with CCMP and NOAA wind data to study the wind effects on the drifter-inferred velocities. It was found that the difference between simultaneous and quasi-collocated drogued and undrogued SVP velocities, which is an underestimate of the slippage of the undrogued SVP drifter, amounts about 1.4% of the wind speed and is mainly downwind. In other words, undrogued SVP drifters have a downwind leeway of at least 14 cm/s in 10 m/s winds. This result, is higher than the one found by Poulain et al. (2009), which was 0.66% of the wind speed.

9. Study on the Stokes drift velocities

Stokes drift velocities at the location of the pairs of drogued undrogued drifters were computed. The following scatter diagram, Figure 9, shows the Stokes drift velocities versus wind speed at the locations and times of the pairs considered in the Mediterranean Sea.

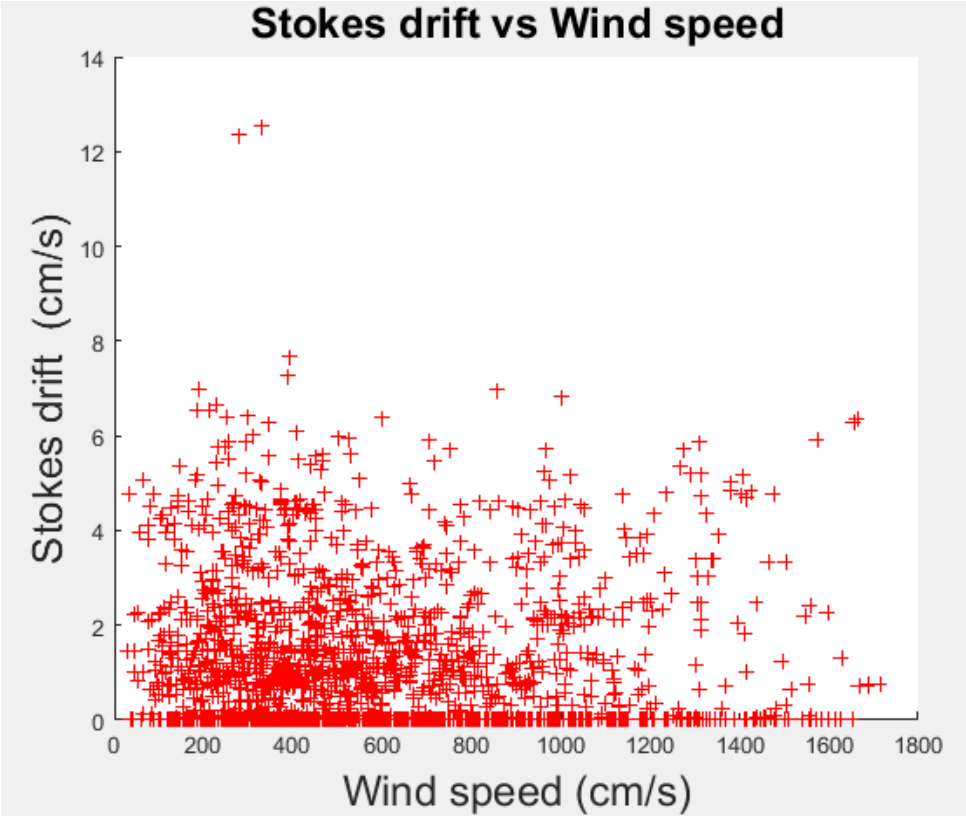

Figure 9. Scatter diagram of Stokes drift velocities vs wind speed at the drifter pair locations and times.

Stokes drift velocities at the pair locations are ranging between 0 and 12 cm/s. In addition, there can be Stokes drift velocities even if there is no or little wind, it is the case when there is swell.

Figures 10a and 10b show the Stokes drift velocity vs the wind speed at all the grid points (see Figure 3) in the western Mediterranean basin. Figures 10c and 10d show the same results but for the easter basin. According to these four figures we can notice that waves with a significant height under 1 m induced only low Stokes drift velocities, around 2 cm/s. In contrast, when the wave significant height is over 1 m, Stokes drift velocities can reach 10 cm/s in both western and eastern basins.

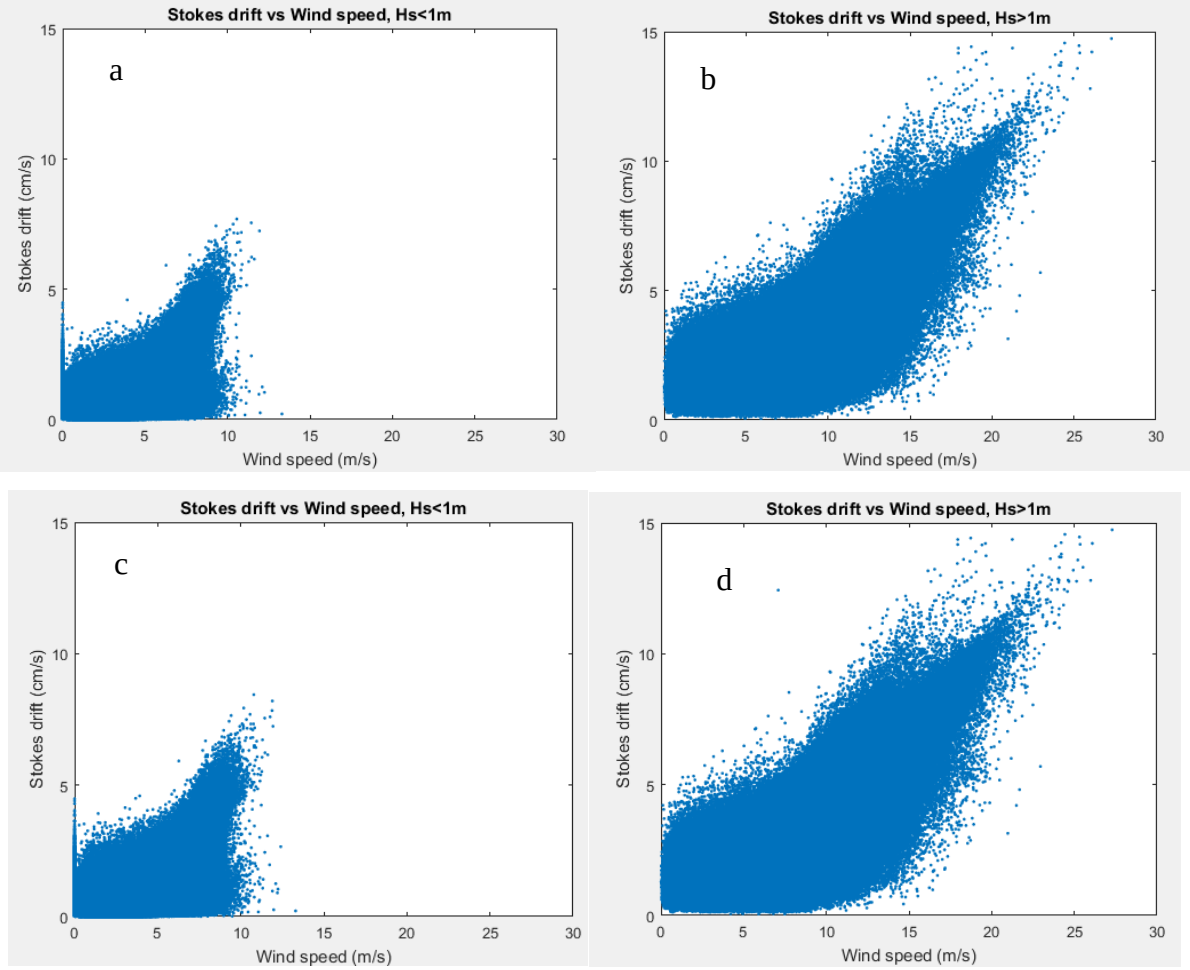

Figure 10. Scatter diagram of Stokes drift velocities vs wind speed in the western (a and b) and eastern (c and d) basins as a function of the significant height.

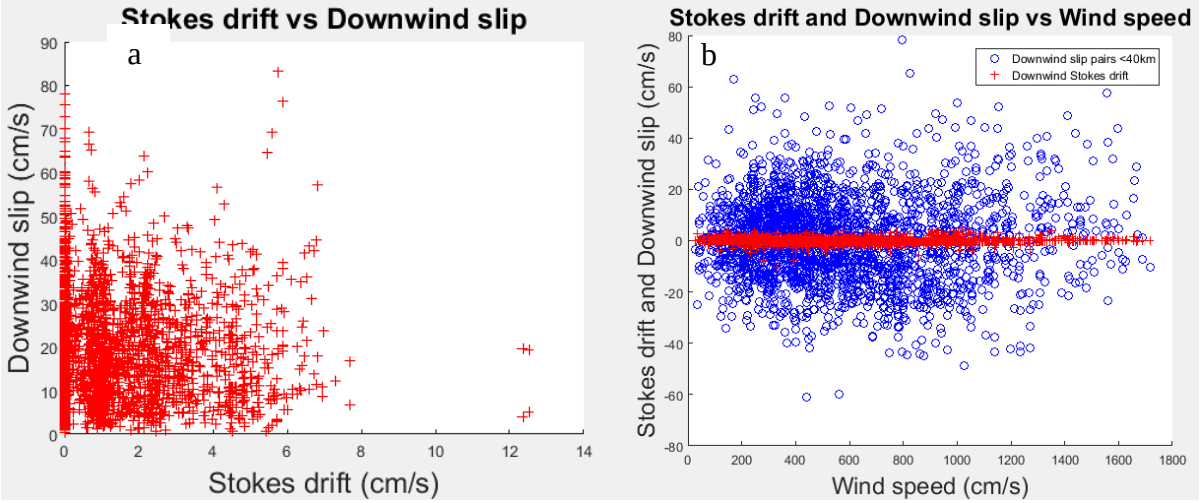

Figure 11 a) Scatter diagram of Stokes drift velocities vs downwind slip; b) Scatter diagram of downwind Stokes drift and downwind slip velocities vs wind speed.

The Stokes drift velocity vs downwind slip is depicted in Figure 11a and the downwind Stokes drift velocity and slip vs wind speed is plotted in Figure 11b. It shows that the range of Stokes drift velocities is very small compared to the range of the downwind slip velocities and that the downwind slip is almost always superior to the Stokes drift velocity.

10. Conclusions

According to the above results, the wind-driven currents seem to have a higher influence than the waves on the drifter trajectories. Indeed, a 10 m/s wind speed would induce a wind-driven current of the drifter of about 14 cm/s in the downwind direction, whereas the Stokes drift influence would be only about 2-10 cm/s. In addition, the results found by Poulain and al. (2009) have been updated using a more copious drifter dataset. Results show that the slippage of the SVP drifter without drogue is essentially downwind and amounts for about 1.4% of the wind speed.

11. References

Ardhuin, F. and J.-F. Filipot, 2017. Ocean wave in geosciences. Technical Report.
Doi: 10.13140/RG.2.2.28981.78562

Atlas, R., Ardizzone, J. V., Hoffman, R., Jusem, J. C., and Leidner, S. M., 2009. Cross calibrated, multi-platform ocean surface wind velocity product (MEaSUREs Project), Guide Document, Physical Oceanography Distributed Active Archive Center (PO.DAAC), JPL, Pasadena, California, Version 1.0., 26 pp.

Besio, G., Briganti, R., Romano, A., Mentaschi, L. & De Girolamo, P. 2017. Time clustering of wave storms in the Mediterranean Sea *Natural Hazards Earth System Science*, **17**, pp. 505-514, doi:10.5194/nhess-17-505-2017

Besio G., Mentaschi L.& Mazzino A., 2016. Wave energy resource assessment in the Mediterranean Sea on the basis of a 35-year hindcast *Energy*, **94**, pp. 50-63 doi:10.1016/j.energy.2015.10.044

Davis, R. E., 1985: Drifter observation of coastal currents during CODE.
Doi: http://falk.ucsd.edu/reading/davis_jgr85b.pdf

Hansen, D.V. and A. Herman, 1989. Temporal sampling requirements for surface drifting buoys in the tropical Pacific. Journal of Atmospheric and Oceanic Technology, 6, 588-607.

Hansen, D. V. and P.-M. Poulain, 1996. Processing of WOCE/TOGA drifter data. Journal of Atmospheric and Oceanic Technology, 13, 900-909.

Heath N., 2011, Determining the Effects of Stokes Drift on the Movement of Oil in the Gulf of Mexico.
Doi: http://citeseerx.ist.psu.edu/viewdoc/summary?doi=10.1.1.363.4059

Jordà, G., R. Bolaños, M. Espino, and A. Sànchez-Arcilla, 2007: Assessment of the importance of the current-wave coupling in the shelf ocean forecasts.
Doi: https://www.ocean-sci.net/3/345/2007/os-3-345-2007.pdf

Kumar N., Cahl D. L., Crosby S. C. And Voulgaris G., 2017. Bulk versus spectral wave parameters : implications on stokes drift estimates, regional wave modeling and HF radars applications.
Doi : http://journals.ametsoc.org/doi/pdf/10.1175/JPO-D-16-0203.1

Masina, M., Archetti, R., Besio, G. & Lamberti, A. 2017. Tsunami taxonomy and detection from recent Mediterranean tide gauge data *Coastal Engineering*, **127**, pp. 145-169, doi:10.1016/j.coastaleng.2017.06.007

Mentaschi L., Besio G., Cassola F. & Mazzino A., 2013. Problems in RMSE-based wave model validations. *Ocean Modelling*, **72**, pp. 53-58 doi:10.1016/j.ocemod.2013.08.003

Mentaschi L., Besio G., Cassola F. & Mazzino A., 2013. Developing and validating a forecast/hindcast system for the Mediterranean Sea. *Journal of Coastal Research*, **SI 65**, pp. 1551-1556.

Mentaschi L., Perez J., Besio G., Mendez F. & Menendez M., 2015. Parameterization of unresolved obstacles in wave modeling: a source term approach. *Ocean Modelling*, **96**, pp. 93-102 doi:10.1016/j.ocemod.2015.05.004

Mentaschi L., Besio G., Cassola F. & Mazzino A., 2015. Performance evaluation of WavewatchIII in the Mediterranean Sea. *Ocean Modelling*, **90**, pp. 82-94 doi:10.1016/j.ocemod.2015.04.003

Poulain, P. M., Gerin R., Mauri E. and Pennel R., 2009: Wind effects on drogued and undrogued drifters in the Eastern Mediterranean.
Doi : http://journals.ametsoc.org/doi/pdf/10.1175/2008JTECHO618.1

Sartini L., Mentaschi L. & Besio G., 2015. Comparing different extreme wave analysis models for wave climate assessment along the Italian coast. *Coastal Engineering*, **100**, pp. 37-47 doi:10.1016/j.coastaleng.2015.03.006

Sartini L., Cassola F. & Besio G., 2015. Extreme waves seasonality analysis: an application in the Mediterranean Sea. *Journal of Geophysical Research – Oceans*, **120**, (9), pp. 6266-6288 doi:10.1002/2015JC011061

Sartini, L., Besio, G., Dentale, F. & Reale, F. 2016. Wave Hindcast Resolution Reliability for Extreme Analysis *26th ISOPE - International Ocean and Polar Engineering Conference*, Rhodes, June 26-July 1, pp. 1319-1325

Sybrandy, A. L., and P. P. Niiler, 1991: WOCE/TOGA Lagrangian drifter construction manual. SIO REF 91/6, WOCE Rep.63, Scripps Institution of Oceanography, San Diego, CA, 58pp.

Tolman, H. L., M. Accensi, H. Alves, F. Ardhuin, J. Bidlot, N. Booij, A.-C. Bennis, T. Campbell, D. V. Chalikov, A. Chawla, J.-F. Filipot, M. Foreman, P. Janssen, F. Leckler, Jian-Guo, K. L. M. Orzech, R. Padilla-Hern andez, W. E. Rogers, A. Rawat, A. Roland, M. D. Sikiric, M. Szyszka, H. L. Tolman, B. Tracy, G. P. van Vledder, A. van der Westhuysen, and S. Zieger, 2014: User manual and system documentation of WAVEWATCH-IIITM version 4.18. Technical Report 316, NOAA/NWS/NCEP/MMAB.

Wang, Z., Wu K., Dong S., Deng Z., and Zhang X., 2014: Effect of wave induced Stokes drift on the dynamics of ocean mixed layer.
Doi : https://link.springer.com/article/10.1007/s00343-015-4036-7

Zughayer, R., Gudmestad, O. De Leo, F. & Besio, G. 2017 Metocean Extreme Estimations: The Sensitivity of Offshore Design Measures to Statistics' Uncertainties *27th ISOPE - International Ocean and Polar Engineering Conference*, San Francisco, June 25-30, Vol. III pp. 9-15